An experimental and theoretical investigation of the molecular and electronic structure of 2-amino-4-chloro-6-pyrazolyl-[1,3,5]triazine, forming supramolecular linear tapes in the solid state†‡

Maurizio Casarin,[a] Federica Garau,[a] Magda Monari,*[b] Luciano Pandolfo,*[a] Claudio Pettinari*[c] and Alfonso Venzo[d]

Received (in Montpellier, France) 20th July 2007, Accepted 25th October 2007
First published as an Advance Article on the web 7th November 2007
DOI: 10.1039/b711136c

The new derivative 2-amino-4-chloro-6-pyrazolyl-[1,3,5]triazine, **1**, prepared by reaction of 2-amino-4,6-dichloro-[1,3,5]triazine with an excess of pyrazole, has been characterized by ^{1}H, ^{13}C and ^{15}N NMR measurements and single crystal XRD structural determination. The non-equivalence of the NH_2 hydrogens evidences the iminium character of this moiety. Compound **1**, exploiting strong H-bonds, self-assembles generating supramolecular linear tapes. Theoretical calculations are in good agreement with experimental solid state and solution data. Electronic properties of **1** (lowest lying excitation energies and corresponding oscillator strength) have also been determined by time dependent DFT at the PBE level.

Introduction

Supramolecular chemistry, the "chemistry of molecular assemblies and of the intermolecular bond"[1] is a vast interdisciplinary topical field of research and technology in contemporary chemistry. H-bonding, metal–ligand coordination, and π–π interactions are the noncovalent motifs mainly involved in the rational design of supramolecular assemblies.[2] The prevalent strategy for engineering the structures of crystals takes advantage of directional intermolecular interactions as the main way of controlling molecular assembly during crystallization.[3] H-bonds exhibiting high directionality with respect to other noncovalent interactions,[4] and being generally stronger than the strongest van der Waals (vdW) interaction,[5] are largely employed to design and obtain self-assembled supramolecular organic structures.[6]

Besides carboxylic acids and amides, that easily form robust architectures *via* O–H···O=C,[7] and N–H···O=C[8] interactions, other H-bonding motifs, such as those involving the cyanuric acid–melamine system and, more generically, [1,3,5]triazine derivatives, have proven their great potential in crystal engineering,[9] and *s*-triazine-containing molecules are involved in new developments in the field of functional materials.[10] As an example, by using substituted melamines and barbituric acids, Whitesides and coworkers created a variety of supramolecular motifs through intermolecular H-bonds, such as linear tapes, crinkled tapes and rosette motifs.[11] In linear tapes (infinite, quasi-1D arrangements of molecules held together by multiple noncovalent interactions) each molecule forms H-bonds with only two neighbouring molecules.[12] These tapes are expected to pack with their long axes parallel, further limiting possible orientations of molecules in the solids.[13] These assemblies are expected to be quite stable, due to the high number of H-bonds involved and their relatively high strength.

Other "tapes", based on [1,3,5]triazine derivatives have been reported,[14,15] and also the simple 2-amine-4,6-dichloro-[1,3,5]triazine self-assembles through H-bonds forming in the solid state a series of intercalated tapes, all running along one crystallographic direction.[16,17] Two examples are sketched in Chart 1.

In the synthesis of numerous compounds bearing the *s*-triazine core, 2,4,6-trichloro-[1,3,5]triazine has been largely

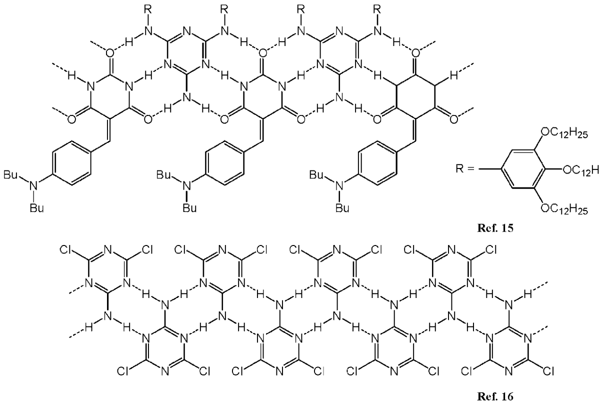

Chart 1

---

[a] Dept. of Chemical Sciences, University of Padova, Via Marzolo, 1, I-35131 Padova, Italy. E-mail: luciano.pandolfo@unipd.it; Fax: +39 049 8275161; Tel: +39 049 8275157

[b] Dept. of Chemistry "G. Ciamician", University of Bologna, Via Selmi, 2, I-40126 Bologna, Italy. E-mail: magda.monari@unibo.it; Fax: +39 051 2099456; Tel: +39 051 2099559

[c] Dept. of Chemical Sciences, Via S. Agostino, 1, University of Camerino, I-62032 Camerino (MC), Italy. E-mail: claudio.pettinari@unicam.it; Fax: +39 0737 637345; Tel: +39 0737 402234

[d] CNR – ISTM University of Padova, Via Marzolo, 1, I-35131 Padova, Italy

† The HTML version of this article has been enhanced with colour images.

‡ Electronic supplementary information (ESI) available: Charts S1 and S2, Scheme S1, Table S1, Fig. S1–S8. See DOI: 10.1039/b711136c

used as a starting material, due to its particular reactivity. Selective syntheses of mono, di and trisubstituted *s*-triazine derivatives could generally be achieved by following *Moffat's rule*:[18] the nucleophilic substitution of the first chloride can be carried out around 0 °C, while the second takes place at r.t., and the third requires temperatures higher than 60–80 °C (Scheme S1‡). As far back as the 19th century[19,20] to nowadays,[21] numerous *s*-triazine containing compounds, having useful applications in disparate fields, have been obtained.[22–25] More recently, *s*-triazine derivatives have been employed in combinatorial chemistry,[26] crystal engineering[11,16,17,27–29] and as ligands.[10,21b,22a,30] Here we report the synthesis of the asymmetric [1,3,5]triazine derivative, 2-amino-4-chloro-6-pyrazolyl-[1,3,5]triazine, **1**, as well as a combined experimental and theoretical study on its structure and solid state supramolecular self-assembly that generates linear tapes by exploiting strong H-bonds.

Experimental

Material and methods

All reactions and manipulations were carried out under an atmosphere of nitrogen with standard Schlenk or septum/cannula techniques. All solvents were purified by conventional methods[31] and stored under nitrogen. Reagents (Aldrich) were used without further purification. Elemental analyses (C, H, N) were performed with a Fisons Instruments 1108 CHNS-O Elemental Analyser. IR spectra were recorded from 4000 to 400 cm^{-1} with a Perkin-Elmer 983 instrument. UV-Vis spectra were recorded from 200 to 800 nm with a Varian Cary 5E instrument.

NMR experimental section

^{1}H, ^{13}C and ^{15}N NMR spectra were obtained as DMSO-d_6 solutions on a Bruker DRX-400 spectrometer operating at 400.13, 100.61 and 40.56 MHz, respectively, and equipped with a BVT2000 temperature controller. The chemical shift values are given in δ units with reference to Me_4Si for ^{1}H and ^{13}C, and $MeNO_2$ for ^{15}N. The assignments are according to the labelling scheme reported in Chart S1.‡ Suitable integral values for the proton spectra were obtained by a pre-scan delay of 10 s to ensure a complete relaxation for all the resonances. The proton assignments were performed by standard chemical shift correlations as well as by 2D correlation spectroscopy (COSY), total correlation spectroscopy (TOCSY), and nuclear Overhauser enhancement spectroscopy (NOESY) experiments. The ^{13}C and ^{15}N chemical shift values were obtained through 2D-heteronuclear correlation experiments (heteronuclear multiple quantum correlation, HMQC), with bilinear rotation-decoupling, BIRD, sequence[32] and quadrature along F1 achieved using the time-proportional receiver phase incrementation, TPPI, method[33] for the H–bonded carbon and nitrogen atoms, and heteronuclear multiple bond correlation, HMBC,[34] for the other ^{13}C and ^{15}N nuclei.

Computational details

ADF calculations on **1** have been carried out by using the ADF 2006–2007 package.[35] Optimized geometries were obtained by employing generalized gradient (GGA) corrections self-consistently included through the Perdew–Burke–Ernzerhof (PBE) formula.[36] A triple-ζ Slater-type basis set was used for all the atoms of the molecule. Inner cores of C(1s), N(1s) and Cl(1s2s2p) atoms have been kept frozen throughout the calculations. All the numerical experiments have been run without the assumption of any symmetry element (C_1 symmetry point group). The optimized structure was then used to calculate NMR isotropic shielding constants (σ). Chemical shifts were evaluated as $\delta = \sigma_{\mathrm{ref}} - \sigma$, where σ_{ref} is the shielding constant of ^{1}H in the reference compound (TMS). Finally, lowest lying excitation energies and corresponding oscillator strengths have been computed by employing time dependent density functional theory (TD-DFT).[37]

Synthesis

2-Amino-4-chloro-6-pyrazolyl-[1,3,5]triazine, 1. To a stirred solution of 2-amino-4,6-dichloro-[1,3,5]triazine[19] (301 mg, 1.8 mmol) and DIPEA (*N*,*N'*-diisopropylethylamine, 0.6 mL, 0.47 g, 3.6 mmol) in dioxane (10 mL) a solution of pyrazole (Hpz) (254 mg, 3.7 mmol) in dioxane (8 mL) was added dropwise. The mixture was refluxed for 10 h, obtaining an orange solution and the solvent was then removed under reduced pressure. The resulting orange solid was vigorously stirred with 20 mL of water at r.t. for 1 h giving a white solid that was filtered, washed with water and dried under vacuum. Yield 286 mg. ^{1}H NMR of the crude product indicated the presence of *ca.* 80% of **1**, that was recrystallized from MeOH, yielding a few white crystals suitable for X-ray crystal structure determination.

1: Mp > 200 °C. Anal.(%) Calcd. for $C_6H_5N_6Cl$: C, 36.66; H, 2.56; N, 42.75. Found: C, 36.82; H, 3.47; N, 37.78. IR (KBr) cm^{-1}: 3480; 3323; 3160; 1633; 1575; 1523; 1449; 1396; 1324; 1007. ^{1}H NMR (δ, DMSO-d_6, 25 °C): NH 8.30, 8.39, H_1 7.87 (dd, $^3J_{\mathrm{HH}}$, 1.4 Hz; $^4J_{\mathrm{HH}}$, 0.7 Hz), H_2 6.58 (dd, $^3J_{\mathrm{HH}}$, 2.8 Hz; $^3J_{\mathrm{HH}}$, 1.4 Hz), H_3 8.48 (dd, $^3J_{\mathrm{HH}}$, 2.8 Hz; $^4J_{\mathrm{HH}}$, 0.7 Hz). ^{13}C NMR (δ, DMSO-d_6, 25 °C) C_1 145.11, C_2 110.16, C_3 130.51, C_5 170.39, C_6 161.98, C_4 168.03. ^{15}N NMR (δ, DMSO-d_6, 25 °C) N_6 −274.7, $N_{3(4)}$ −175.6, N_1 −153.6, $N_{4(3)}$ −148.0, N_2 −69.8.

Crystallographic data collection and structure determination. The X-ray intensity data for **1** were measured on a Bruker Apex II CCD diffractometer. Cell dimensions and the orientation matrix were initially determined from a least-squares refinement on reflections measured in three sets of 20 exposures, collected in three different ω regions, and eventually refined against all data. A full sphere of reciprocal space was scanned by 0.3° ω steps. The software SMART[38] was used for collecting frames of data, indexing reflections and determination of lattice parameters. The collected frames were then processed for integration by the SAINT program,[38] and an empirical absorption correction was applied using SADABS.[39] The structure was solved by direct methods (SIR 97)[40] and subsequent Fourier syntheses and refined by full-matrix least-squares on F^2 (SHELXTL),[41] using anisotropic thermal parameters for all non-hydrogen atoms. All hydrogen atoms were located in the Fourier map and, except the iminic hydrogens which were refined isotropically, added in calculated positions, included in the final stage of refinement with isotropic thermal parameters, $U(\mathrm{H}) = 1.2U_{\mathrm{eq}}(\mathrm{C})$, and allowed to ride on their carrier carbons. The absolute structure was determined [Flack parameter −0.03(4)]. Crystal data and details of data collection for **1** are reported in Table 1. CCDC reference number 662889. For crystallographic data in CIF or other electronic format see DOI: 10.1039/b711136c

Molecular graphics were generated using Mercury[42] and SCHAKAL[43] software.

Results and discussion

In the course of our search of polynucleating ligands able to generate metal–organic frameworks, we directed our attention to the potential of the [1,3,5]triazine supramolecular synthon and started our study from the relatively simple *s*-triazine derivative **1**. Actually, **1** was first obtained during an attempt to synthesize 2-amino-4,6-dipyrazolyl-[1,3,5]triazine. Workup of the mixture obtained by refluxing 2-amino-4,6-dichloro-[1,3,5]triazine with 2 equivalents of Hpz in dioxane for 10 h, yielded only *ca.* 20% of 2-amino-4,6-dipyrazolyl-[1,3,5]triazine and *ca.* 80% of **1**, as indicated by ^{1}H NMR spectroscopy and elemental analysis. Nevertheless, it was possible to recrystallize **1** from MeOH obtaining some crystals that were used for a single crystal XRD structural determination and ^{1}H, ^{13}C and ^{15}N NMR measurements.

The molecular structure of **1** is shown in Fig. 1 and relevant bond lengths and angles are reported in Table 2.

The molecule is almost completely planar, with the plane of the triazine ring forming a dihedral angle of *ca.* 9° with the plane of the pyrazolate ring. The [1,3,5]triazine ring shows significant distortions from regular hexagonal geometry due to the steric effects of the lone pair electrons as it has been found in the case of *s*-triazine.[44] The inner C–N–C angles are in the range 111.5–113.5(1)° (av. 112.7°) whereas the N–C–N angles fall in the range 124.6–129.3(1)° (av. 127.3°). These differences between C–N–C and N–C–N angles are even more marked than those found in the parent *s*-triazine [C–N–C 113.0(2)° and N–C–N 127.0(2)°].[44]

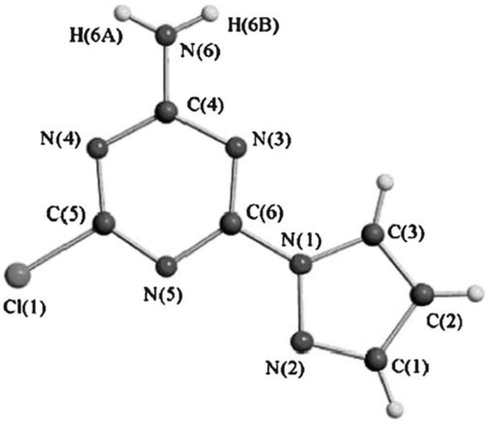

Fig. 1 Molecular structure of **1**.

The X-ray crystal structure shows that the geometry around N(6) is, in very good approximation, trigonal planar, with the nitrogen atom approximately lying in the plane formed by H(6A), H(6B) and C(4) (deviation from plane 0.06 Å). The C(4)–N(6) bond length [1.321(2) Å] well compares with the N(3)–C(6) and N(4)–C(5) distances [1.319(2) and 1.307(2) Å, respectively], while it is shorter than the C(4)–N(3) and C(4)–N(4) ones [1.351(2) and 1.357(2) Å, respectively]. These data, in very good agreement (Table S1‡) with the optimized geometrical parameters of **1**, determined by DFT calculations at the PBE level, suggest a relevant iminium character of the NH_2 fragment (see also Chart S2‡). Computed Hirshfeld charges of N(3) (−0.1836), N(4) (−0.1941), N(5) (−0.175) and N(6) (−0.144) further support this finding.

An inspection of the crystal packing reveals that each molecule of **1** is involved in infinite supramolecular linear tapes due to N–H···N and N–H···Cl hydrogen bonds established by the iminic hydrogens [H(6A), H(6B)] (Fig. 2). The

Table 1 Crystal data and details of data collection for compounds **1**

Compound	**1**
Formula	$C_6H_5ClN_6$
Formula weight	196.61
T/K	293(2)
λ(MoKα)/Å	0.71073
Crystal symmetry	Monoclinic
Space group	*Pc*
a/Å	4.2896(5)
b/Å	5.4645(6)
c/Å	17.528(2)
α/°	90
β/°	91.449(2)
γ/°	90
V/Å^3	410.72(8)
Z	2
ρ_{calc}/Mg m^{-3}	1.590
μ(Mo-Kα)/mm^{-1}	0.423
F(000)	186
Crystal size/mm	0.15 × 0.20 × 0.30
θ range/°	3.73–28.50
Reflections collected	3337($\pm h$, $\pm k$, $\pm l$)
Unique observed reflections [$F_o > 4\sigma(F_o)$]	1848 [$R_{\mathrm{int}} = 0.0153$]
Goodness-of-fit-on F^2	1.094
Final *R* indices $I > 2\sigma(I)$	$R_1(F)^a = 0.0261$, $wR_2(F^2)^b = 0.0696$
R indices (all data)	$R_1(F) = 0.0270$, $wR_2 = 0.0699$
Largest diff. peak and hole/e Å^{-3}	0.152 and −0.219

[a] $R_1 = \Sigma||F_o| - |F_c||/\Sigma|F_o|$. [b] $wR_2 = [\Sigma w(F_o^2 - F_c^2)^2/\Sigma w(F_o^2)^2]^{1/2}$ where $w = 1/[\sigma^2(F_o^2) + (aP)^2 + bP]$ where $P = (F_o^2 + 2F_c^2)/3$.

Table 2 Bond lengths (Å) and angles (deg) for **1**

Cl(1)–C(5)	1.736(1)	C(4)–N(6)	1.321(2)
N(5)–C(5)	1.323(2)	C(6)–N(1)	1.400(2)
N(5)–C(6)	1.336(2)	C(3)–C(2)	1.354(3)
N(4)–C(5)	1.307(2)	C(3)–N(1)	1.364(2)
N(4)–C(4)	1.357(2)	C(1)–N(2)	1.321(2)
N(3)–C(6)	1.319(2)	C(1)–C(2)	1.390(3)
N(3)–C(4)	1.351(2)	N(1)–N(2)	1.3560(2)
C(5)–N(5)–C(6)	111.5(1)	N(4)–C(5)–N(5)	129.3(1)
C(5)–N(4)–C(4)	113.1(1)	N(4)–C(5)–Cl(1)	116.5(1)
C(6)–N(3)–C(4)	113.5(1)	N(5)–C(5)–Cl(1)	114.3(1)
N(6)–C(4)–N(3)	117.8(2)	C(2)–C(3)–N(1)	106.3(2)
N(6)–C(4)–N(4)	117.6(2)	N(2)–C(1)–C(2)	112.5(2)
N(3)–C(4)–N(4)	124.6(1)	C(3)–C(2)–C(1)	105.4(2)
N(3)–C(6)–N(5)	128.0(1)	N(2)–N(1)–C(3)	112.0(1)
N(3)–C(6)–N(1)	116.4(1)	N(2)–N(1)–C(6)	121.0(1)
N(5)–C(6)–N(1)	115.6(1)	C(3)–N(1)–C(6)	126.9(1)
C(1)–N(2)–N(1)	103.7(2)		

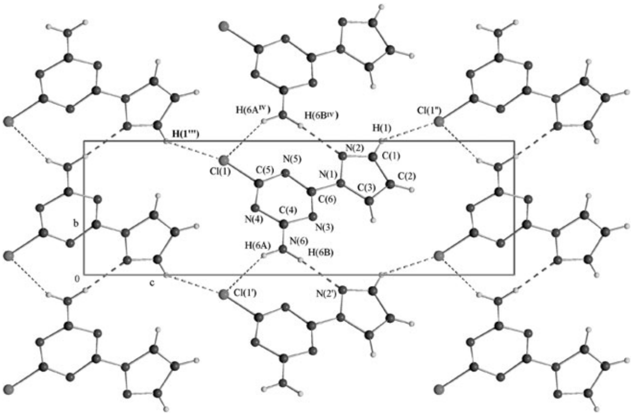

Fig. 2 View down the *a* axis of the crystal packing of **1** showing the intermolecular interactions. Symmetry codes: (I) *x*, 1 − *y*, *z* − 0.5, (II) *x*, 2 − *y*, *z* + 0.5; (III) *x*, 2−*y*, *z*−0.5, (IV) *x*, 1 + *y*, *z*.

H-bond involving H(6B) bound to N(6) of the substituted triazine ring is with the pyrazolate nitrogen N(2) of one neighbour molecule [N(6)···N(2′) 3.012(2) Å, N(6)–H(6B)···N(2′) 172(2)°], whereas the second iminic hydrogen H(6A) interacts with the chlorine atom of the same neighbour (Table 3).

These tapes are arranged in face-to-face π stackings with an interplanar distance of about 3.31 Å (Fig. 3), close to the graphitic one, but with a ring offset of 2.73 Å [centroid(triazine)–centroid(triazine) distance 4.29 Å]. As a consequence of this slippage the shorter interactions are between one nitrogen [N(5)] of the triazine and one nitrogen [N(1)] of the pyrazolate group of one molecule with the carbon [C(4)] bearing the NH_2 moiety and N(3) of the adjacent molecule, respectively [N(5)···C(4^a) 3.34 Å, N(1)···N(3^a) 3.32 Å, symmetry code: (a) *x* + 1, *y*, *z*].

In the overall crystal packing of **1** (Fig. 4) differently oriented columns arising by the π stacking of the molecules form dihedral angles of 75.25(3)°. The columns are mostly connected by van der Waals interactions between the chlorine atoms of one column and one hydrogen of the pyrazole ring [Cl(1)···H(1‴) 2.94 Å, Cl(1)···H(1‴)–C(1‴) 145°, symmetry code as in Fig. 2] of the neighbour (sum of the vdW radii Cl···H = 2.95 Å using the van der Waals radii according to Bondi).[45]

Finally, the PLATON CALC SOLV routine[46] indicates that in solid **1** there are no solvent accessible areas, as suggested also by space-filling views (Fig. S1 and S2‡).

Multinuclear NMR measurements have been carried out on DMSO-d_6 solutions of **1** (see Experimental) giving spectra in agreement with X-ray findings (Fig. S4–S6‡). In particular, ^{1}H,[30b] ^{13}C,[30b] and ^{15}N[47] chemical shift values fall in the typical ranges reported for similar compounds.

Table 3 Hydrogen bonding interactions in **1**[a]

D–H···A	D–H/Å	H···A/Å	D···A/Å	D···A/°
N(6)···N(2′)	0.85(2)	2.17(2)	3.012(2)	172(2)
N(6)···Cl(1′)	0.86(2)	2.89(2)	3.660(2)	150(2)

[a] Symmetry transformations: (I) *x*, 1 − *y*, *z* − 0.5.

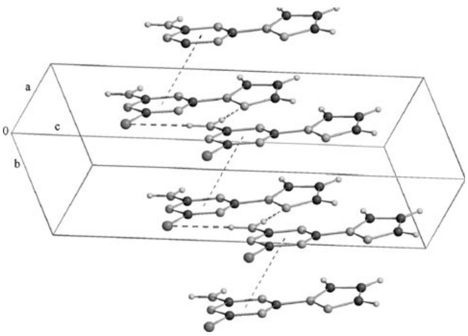

Fig. 3 Simplified crystal packing of **1** showing the offset π stacking of the triazine rings between pairs of molecules.

^{1}H NMR chemical shifts of **1** have also been estimated by carrying out numerical experiments at both the Becke–Perdew (BP) and PBE levels and the results are reported in Table 4.

Despite the fact that the calculated values pertinent to H(1), H(2) and H(3) for isolated **1** are in very good agreement with experimental data, those evaluated for H(6A) and H(6B) are rather poor. On the other hand, it is useful to keep in mind that the spectra were recorded in DMSO-d_6, and it is well known that this solvent breaks H-bonds and can form new ones involving the NH_2 moiety. On this basis, we decided to evaluate the ^{1}H chemical shifts of a hypothetical adduct formed by one molecule of **1** and two molecules of DMSO. The optimized geometry of the adduct (Fig. S3‡) was obtained by using a triple-ζ Slater-type basis set for the O and S atoms and by freezing the inner cores of O(1s) and S(1s2s2p) throughout the calculations. The agreement between experiment and theory resulting was definitely better, particularly for the PBE functional.

The most relevant feature evidenced in the ^{1}H NMR spectrum of **1** (Fig. S4‡) is the non equivalence of the two NH_2 hydrogens (two distinct signals at 8.30 and 8.39 ppm).[48] These data, supported also by theoretical results, indicate that the rotation around the C(4)–NH_2 bond is hindered, thus

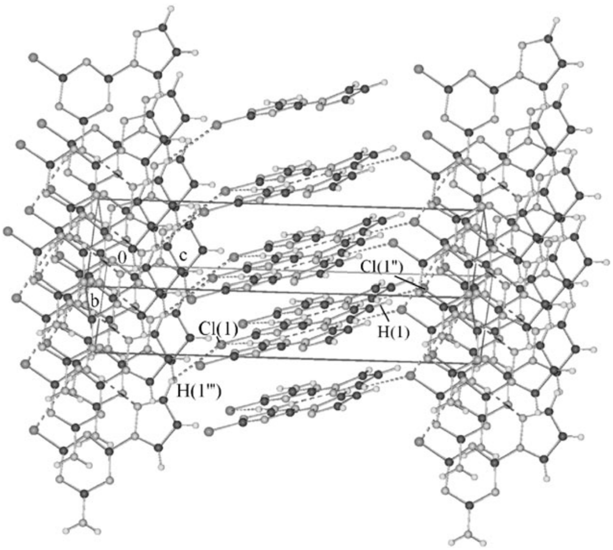

Fig. 4 Arbitrary view of the packing of **1** showing the differently oriented parallel rows of tapes. Symmetry codes as in Fig. 2.

Table 4 Calculated and experimental ^{1}H NMR chemical shifts of **1**. Atoms are labeled according to Chart S1‡

	Isolated **1**		$\mathbf{1}\cdot 2$DMSO adduct		
	BP	PBE	BP	PBE	Exp
H(1)	7.76	7.63	7.76	7.55	7.63
H(2)	6.72	6.53	6.60	6.42	6.53
H(3)	8.86	8.66	8.94	8.72	8.63
H(6A)	5.20	5.00	8.60	7.71	8.39
H(6B)	5.10	4.91	7.47	7.03	8.30

confirming the importance of the resonance iminium formula (Chart S2‡) already evidenced by the X-ray crystal structure analysis. It is important to point out that the hindered rotation cannot be due to the participation of the NH_2 group to the intermolecular H-bonds (*vide supra*) that should be completely broken in DMSO-d_6 solution.

In order to obtain an evaluation of the rotational barrier around the C(4)–N(6) bond, we registered 1D ^{1}H NMR and 2D-EXSY (exchange spectroscopy) spectra at different temperatures, in the range 298–328 K. Qualitatively, we observed the beginning of the coalescence of the two N–H signals at 328 K, while the rate constant values for the exchange of H(6A) and H(6B) (Fig. 5) were evaluated by integrating the diagonal peaks and cross-peaks of the 2D-EXSY spectrum.[49]

The activation energy (E_a) of the exchange process resulting from an Arrhenius plot[50] (Fig. 5) amounts to E_a = 119 kJ mol^{-1}. The rotational barrier around the C(4)–N(6) bond was also theoretically estimated. We computed the binding energy (BE) of **1** as a function of torsion angle H(6B)–N(6)–C(4)–N(3) (Θ) by scanning Θ from 0° to 180° at 15° steps, without any geometrical optimization, obtaining a maximum for $\Theta = 90°$ (see Fig. S7‡). The rotational barrier was evaluated as the difference between the maximum value of binding energy of the structure ($\Theta = 90°$) and that of the ground state ($\Theta = 0°$ or 180°), obtaining E_a = 99 kJ mol^{-1}, in very good agreement with the value obtained from 2D-EXSY spectra.

From the synthetic point of view, it is also worth noting the lack of reactivity of the NH_2 moiety of **1** with C_3O_2,[51] the anhydride of malonic acid,[52] to give the corresponding diamidic derivative.[53] Such a behaviour, indicative of the unavailability of the nitrogen lone pair on NH_2, again confirms its iminium character.

A further point deserves to be mentioned. Compound **1** is almost completely insoluble in most organic solvents, showing a low solubility only in MeOH (from which it was recrystallized) and in DMSO. Since both solvents are known to break H-bonds, it is likely that insolubility is due to this kind of interaction, as suggested by the X-ray crystal structure determination (*vide supra*). To look into this point, a further series of numerical experiments have been carried out to get a semi-quantitative estimate of the intermolecular H-bond strength involving the N(6)–H(6B) moiety and the pyrazolate N atom of a second molecule.[54]

We examined the dimeric assembly formed through the H-bond interaction between N(6)–H(6B) and N(2′) of another molecule of **1**. This dimer was obtained by translating a single molecule along the axis defined by the C(4)–N(6) bond. The equilibrium distance between the two molecules was obtained by optimizing the structure of the dimeric assembly without any constraint. In this regard, it has to be remarked that calculations were limited to the PBE functional because it is well known that it provides quite good results when H-bonds are involved.[55,56] The calculated equilibrium distance between the two monomers is in reasonable agreement with experimental data [N(5′)–N(6): calcd. = 3.154 Å, expt. = 2.945 Å; N(6)–N(2′): calcd. = 3.003 Å, expt. = 3.013 Å; N(6)–H(6B)–N(2′): calcd. = 175.80°, expt. = 171.45°]. Furthermore, the ($E_D - 2E_M$) stabilization energy[57] corrected for the preparation energy (the energy required to relax the structure of the free monomers to the geometry they assumed in the dimer), and basis set superposition error (BSSE)[58] amounts to 34.3 kJ mol^{-1}. Strictly speaking, this stabilization derives also from the N(6)–H(6A)···Cl(1′) weak interaction[54] but it is very likely that its contribution is negligible[59] with respect to the N(6)–H(6B)···N(2′) H-bond. It is noteworthy that the calculated stabilization energy value is similar to that reported for O=C–OH···O=C–OH interactions in carboxylic acids.[5a]

Finally, we evaluated the lowest lying excitation energies and corresponding oscillator strengths of **1** by employing time dependent DFT at the PBE level. Calculated transition energies are in good agreement with the experimental values

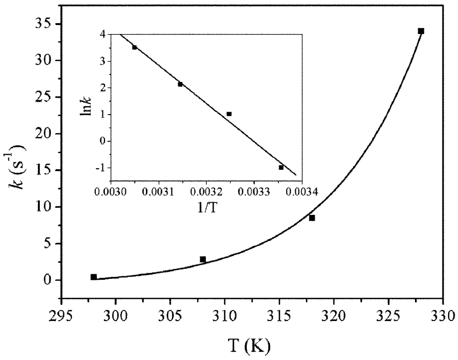

Fig. 5 Rate constant k for the exchange of H(6A) and H(6B) as a function of T. The inset accounts for the corresponding Arrhenius plot.

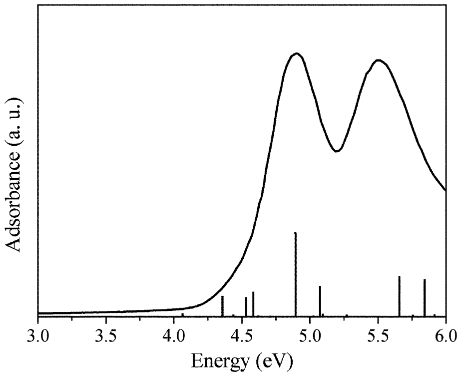

Fig. 6 Experimental UV-Vis spectrum of **1**. Vertical bars represent the theoretical oscillator strength values (*f*) obtained by TD-DFT calculations.

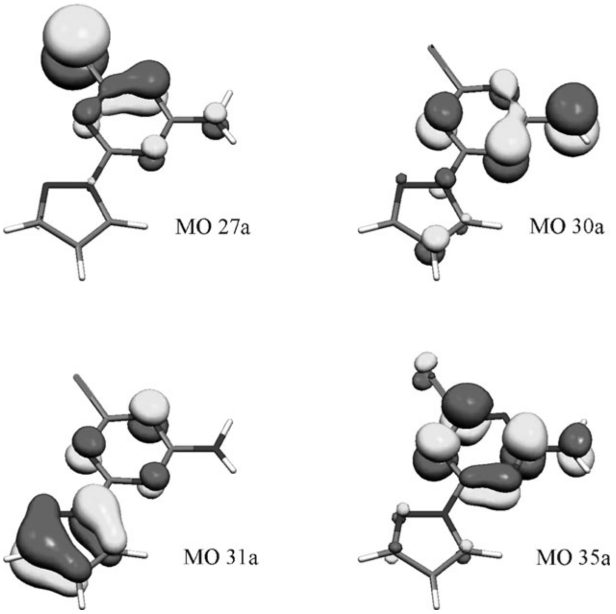

Fig. 7 3D contour plots of MO exited configurations generating UV-Vis spectrum of **1**.

obtained from UV-Vis spectrum in MeOH solution (see Fig. 6).

Both bands are generated by a significant mixing of excited configurations. In particular, to the lowest lying band, (4.89 eV, expt. 4.90 eV) the excited configurations 31a → 35a, 31a → 34a and 27a → 34a contribute 57%, 24% and 11%, respectively, while, as far as the latter band (5.66 eV; expt. 5.51 eV) is concerned, the 30a → 35a excited configuration contributes to it 68%. In Fig. 7 are shown the 3D contour plots of above indicated MOs.

Interestingly, transitions bearing a significant contribution from the HOMO → LUMO (33a → 34a) excited configuration (Fig. S8‡) are all characterized by very low oscillator strength values.

Conclusions

We have reported that the reaction of 2-amino-4,6-dichloro-[1,3,5]triazine with 2 equivalents of Hpz at 100 °C yields a mixture containing only *ca.* 20% of the fully substituted product 2-amino-4,6-dipyrazolyl-[1,3,5]triazine and *ca.* 80% of the di-substituted 2-amino-4-chloro-6-pyrazolyl-[1,3,5]triazine, **1**. This finding indicates that the *Moffat's rule*[18] is to be considered only as a qualitative indication, the reactivity of monosubstituted derivatives largely depending on the effect of the first introduced substituent. In our case, the presence of the NH_2 group strongly deactivates[60] the system towards the introduction of two pyrazolates, thus yielding prevalently **1** even in drastic reaction conditions.

In any case, compound **1** forms a new, robust supramolecular linear tape, whose formation is exclusively dictated by medium–strong H-bonds, as indicated not only by geometrical parameters but also by the calculated stabilization energy, of *ca.* 34.3 kJ mol^{-1}.

Even when the H-bonds are broken, as happens in DMSO solution, both experimental findings (^{1}H NMR, the unreactivity of **1** towards C_3O_2[51]) and DFT calculations provide evidence for the iminium character of the NH_2 moiety of **1** and the consequent unavailability of the nitrogen lone pair. This finding is particularly interesting, mainly in view of the possible use of **1** (and similar derivatives) in coordination chemistry. As a matter of fact, this means that the NH_2 of **1** cannot be involved into any metal coordination, analogously to what has been observed with melamine (2,4,6-triamine-[1,3,5]triazine). For the latter, only a few cases of structurally validated metal coordination compounds are reported[61] and melamine always results in bonding like pyridine to the metal centres, with one nitrogen atom of the aromatic ring.[62] On the other hand the NH_2 moiety might be involved in strong H-bonds, thus generating robust networks.

For these reasons our future researches in this field will be focused on the use of **1** (and related compounds) to coordinate metal ions through pyrazolate and/or endocyclic triazine nitrogen(s) while the NH_2 (iminic) moieties will be useful to form H-bonds, thus generating robust MOFs (metal–organic frameworks) by supramolecular interactions.

Acknowledgements

This work was supported by the Italian PRIN funding n. 2006038447. Computational resources and assistance were provided by the "Laboratorio Interdipartimentale di Chimica Computazionale" (LICC) at the Department of Chemical Sciences of the University of Padova. M. M. wishes to thank the University of Bologna for financial support.

References

1 J. M. Lehn, *Pure Appl. Chem.*, 1978, **50**, 871.
2 J. C. Noveron, M. S. Lah, R. E. Del Sesto, A. M. Arif, J. S. Miller and P. J. Stang, *J. Am. Chem. Soc.*, 2002, **124**, 6613.
3 J. C. MacDonald, P. C. Dorrestein, M. M. Pilley, M. M. Foote, J. L. Lundburg, R. W. Henning, A. J. Schultz and J. L. Manson, *J. Am. Chem. Soc.*, 2000, **122**, 11692.
4 K. Ariga and T. Kunitake, *Acc. Chem. Res.*, 1998, **31**, 371.
5 (*a*) T. Steiner, *Angew. Chem., Int. Ed.*, 2002, **41**, 48; (*b*) D. Braga and F. Grepioni, *Acc. Chem. Res.*, 2000, **33**, 601.
6 B. Gong, Y. Yan, H. Zeng, E. Skrzypczak-Jankunn, Y. W. Kim, J. Zhu and H. Ickes, *J. Am. Chem. Soc.*, 1999, **121**, 5607 and references therein.
7 J.-R. Li, Y. Tao, Q. Yu and X.-H. Bu, *Cryst. Growth Des.*, 2006, **6**, 2493.
8 G. Pavlović, V. Tralić-Kulenović, M. Vinković, D. Vikić-Topić, I. Matanović and Z. Popović, *Struct. Chem.*, 2006, **17**, 275.
9 R. Mondal, J. A. K. Howard, R. Banerjee and G. R. Desiraju, *Cryst. Growth Des.*, 2006, **6**, 2507.
10 P. Gamez and J. Reedijk, *Eur. J. Inorg. Chem.*, 2006, 29 and references therein.
11 (*a*) J. A. Zerkowski, J. C. MacDonald and G. M. Whitesides, *Chem. Mater.*, 1994, **6**, 1250; (*b*) J. A. Zerkowski and G. M. Whitesides, *J. Am. Chem. Soc.*, 1994, **116**, 4298; (*c*) J. A. Zerkowski, J. P. Mathias and G. M. Whitesides, *J. Am. Chem. Soc.*, 1994, **116**, 4305; (*d*) J. A. Zerkowski, C. T. Seto, D. A. Wierda and G. M. Whitesides, *J. Am. Chem. Soc.*, 1990, **112**, 9025.
12 (*a*) J. C. MacDonald and G. M. Whitesides, *Chem. Rev.*, 1994, **94**, 2383; (*b*) E. E. Simanek, A. Tsoi, C. C. C. Wang, G. M. Whitesides, M. T. McBride and G. T. R. Palmore, *Chem. Mater.*, 1997, **9**, 1954.

13 S. Palacin, D. N. Chin, E. E. Simanek, J. C. MacDonald, G. M. Whitesides, M. T. McBride and G. T. R. Palmore, *J. Am. Chem. Soc.*, 1997, **119**, 11807.

14 (*a*) Y. Z. Ren, S. G. Chen, X. D. Chai, Y. W. Cao, W. S. Yang, R. Lu, G. Li, A. D. Lu, M. X. Gong, Y. B. Bai, T. J. Li and J. M. Lehn, *Synth. Met.*, 1995, **71**, 1709; (*b*) W. S. Yang, S. G. Chen, X. D. Chai, Y. W. Cno, R. Lu, W. P. Chai, Y. S. Jiang, T. J. Li and J. M. Lehn, *Synth. Met.*, 1995, **71**, 2107.

15 F. Würthner, S. Yao, B. Heise and C. Tschierske, *Chem. Commun.*, 2001, 2260.

16 (*a*) E. A. Archer, N. T. Goldberg, V. Lynch and M. J. Krische, *J. Am. Chem. Soc.*, 2000, **122**, 5006; (*b*) E. A. Archer and M. J. Krische, *J. Am. Chem. Soc.*, 2002, **124**, 5074; (*c*) E. A. Archer, D. F. Cauble, V. Lynch and M. J. Krische, *Tetrahedron*, 2002, **58**, 721.

17 It is noteworthy that this compound exists in a second polymorphic crystal species having a slightly different molecular structure and forming similar tapes assembling in the lattice in a quite different fashion: J. Glaser, S. Tragl and H. J. Meyer, *Z. Kristallogr.*, 2005, **220**, 214.

18 W. W. Cuthbertson and J. S. Moffat, *J. Chem. Soc.*, 1948, 561.

19 O. Diels, *Ber. Dtsch. Chem. Ges.*, 1899, **32**, 695.

20 A. Hofmann, *Ber. Dtsch. Chem. Ges.*, 1886, **19**, 2061.

21 (*a*) E. M. Smolin and L. Rapoport, *s-Triazines and Derivatives*, Interscience Publisher Inc., New York, 1959; (*b*) T. J. Mooibroek and P. Gamez, *Inorg. Chim. Acta*, 2007, **360**, 381 and references therein.

22 (*a*) M. Maekewa, T. Minematsu, H. Konaka, K. Sugimoto, T. Kuroda-Sowa, Y. Suenaga and M. Munakata, *Inorg. Chim. Acta*, 2004, **357**, 3456; (*b*) H. Brückner and M. Wachsmann, *J. Chromatogr., A*, 2003, **998**, 73.

23 A. de la Hoz, A. Díaz-Ortiz, J. Elguero, L. J. Martínez, A. Moreno and A. Sànchez-Migallón, *Tetrahedron*, 2001, **57**, 4397.

24 N. Lyapchenko, C. Eitner, G. Schroeder and B. Brzezinski, *J. Mol. Struct.*, 2004, **690**, 45.

25 G. Giacomelli, A. Porcheddu and L. D. Luca, *Curr. Org. Chem.*, 2004, **8**, 1497.

26 S. M. Khersonsky and Y. T. Chang, *J. Comb. Chem.*, 2004, **6**, 474.

27 (*a*) P. V. Bernhardt and E. J. Hayes, *Inorg. Chem.*, 1998, **37**, 4214; (*b*) L. J. Prins, E. E. Neuteboom, V. Paraschiv, M. Crego-Calama, P. Timmerman and D. N. Reichnoudt, *J. Org. Chem.*, 2002, **68**, 4808.

28 C. T. Seto and G. M. Whitesides, *J. Am. Chem. Soc.*, 1990, **112**, 6409.

29 L. J. Prins, C. Thalacker, F. Würthner, P. Timmerman and D. N. Reinhoudt, *Proc. Natl. Acad. Sci. U. S. A.*, 2001, **98**, 10042.

30 (*a*) A. Gelling, M. D. Olsen, K. G. Orrel, A. G. Osborne and V. Šik, *Inorg. Chim. Acta*, 1997, **264**, 257; (*b*) V. Milata, R. M. Claramunt, P. Cabildo, M. D. Santa, P. Cornago, L. Infantes, F. H. Cano and J. Elguero, *Heterocycles*, 2001, **55**, 905; (*c*) P. de Hoog, P. Gamez, W. L. Driessen and J. Reedijk, *Tetrahedron Lett.*, 2002, **43**, 6783; (*d*) P. Gamez, P. de Hoog, O. Roubeau, M. Lutz, W. L. Driessen, A. L. Spek and J. Reedijk, *Chem. Commun.*, 2002, 1488; (*e*) R. M. Claramunt, P. Cornago, M. Cano, J. V. Heras, M. L. Gallego, E. Pinilla and M. R. Torres, *Eur. J. Inorg. Chem.*, 2003, 2693.

31 D. D. Perrin, W. L. Armarego and D. R. Perrin, *Purification of Laboratory Chemicals*, 2nd edn, Pergamon Press, Oxford, 1980.

32 (*a*) A. Bax and S. Subramian, *J. Magn. Reson.*, 1986, **67**, 565; (*b*) G. Drobny, A. Pines, S. Sinton, D. Weitekamp and D. Wemmer, *Faraday Symp. Chem. Soc.*, 1979, **B33**, 4912.

33 G. Otting and K. Wüthrich, *J. Magn. Reson.*, 1988, **76**, 569.

34 A. Bax and M. F. Summers, *J. Am. Chem. Soc.*, 1986, **108**, 2093.

35 *Amsterdam Density Functional Package, Version 2006–2007*, Vrjie Universiteit, Amsterdam, The Netherlands, 2007.

36 J. P. Perdew, K. Burke and M. Ernzerhof, *Phys. Rev. Lett.*, 1996, **77**, 3865.

37 (*a*) S. J. A. van Gisbergen, J. G. Snijders and E. J. Baerends, *Comput. Phys. Commun.*, 1999, **118**, 119; (*b*) S. J. A. van Gisbergen, *Molecular Response Property Calculations using Time Dependent Density Functional Theory in Chemistry*, Vrije Universiteit, Amsterdam, 1998, p. 190; (*c*) E. K. U. Gross, J. F. Dobson and M. Petersilka, in *Density Functional Theory*, ed. R. F. Nalewajski, Springer, Heidelberg, 1996.

38 *SMART & SAINT Software Reference Manuals, Version 5.051 (Windows NT Version)*, Bruker Analytical X-Ray Instruments Inc., Madison, WI, USA, 1998.

39 G. M. Sheldrick, *SADABS, Program for Empirical Absorption Correction*, University of Göttingen, Germany, 1996.

40 A. Altomare, G. Cascarano, C. Giacovazzo, A. Guagliardi, A. G. G. Moliterni, M. C. Burla, G. Polidori, M. Camalli and D. Siliqi, *Acta Crystallogr., Sect. A: Found. Crystallogr.*, 1996, **52**, C79.

41 G. M. Sheldrick, *SHELXTLplus Structure Determination Package, Version 5.1 (Windows NT Version)*, Bruker Analytical X-Ray Instruments Inc., Madison, WI, USA, 1998.

42 C. F. Macrae, P. R. Edgington, P. McCabe, E. Pidcock, G. P. Shields, R. Taylor, M. Towler and J. van de Streek, *Mercury: Visualization and Analysis of Crystal Structures, J. Appl. Crystallogr.*, 2006, **39**, 453.

43 E. Keller, *SCHAKAL A Computer Program for the Graphic Representation of Molecular and Crystallographic Models*, Institute for Crystallography of the University of Freiburg, Freiburg, Germany, 1997.

44 P. Coppens, *Science*, 1967, **158**, 1577.

45 A. Bondi, *J. Phys. Chem.*, 1964, **68**, 441.

46 A. L. Spek, *PLATON, A Multipurpose Crystallographic Tool*, Utrecht University, Utrecht, The Netherlands, 2003.

47 (*a*) M. Amm, N. Platzer, J. Guilhem, J. P. Bouchet and J. P. Volland, *Magn. Reson. Chem.*, 1998, **36**, 587; (*b*) W. von Philipsborn and R. Müller, *Angew. Chem., Int. Ed. Engl.*, 1986, **25**, 383.

48 The assignment of 8.39 and 8.30 ppm signals in the experimental spectrum to H(A) and H(B), respectively is made only by qualitative comparison with calculated values.

49 C. L. Perrin and T. J. Dwyer, *Chem. Rev.*, 1990, **90**, 935.

50 M. Umetsu, R. Seki, T. Kadota, Z. Y. Wang, T. Adschiri and T. Nozawa, *J. Phys. Chem. B*, 2003, **107**, 9876.

51 F. Garau and L. Pandolfo, unpublished results.

52 O. Diels and B. Wolf, *Ber. Dtsch. Chem. Ges.*, 1906, **39**, 689.

53 (*a*) T. Kappe and E. Ziegler, *Angew. Chem., Int. Ed. Engl.*, 1974, **13**, 491; (*b*) P. Ganis, G. Valle, L. Pandolfo, R. Bertani and F. Visentin, *Biopolymers*, 1999, **49**, 541.

54 XRD shows also that N(6)–H(6A) and chlorine of a second molecule are likely engaged in a very weak interaction [H(6A)$\cdots$ Cl(1′) 2.90(2) Å, N6–H(6A)$\cdots$Cl(1′) 3.660(1) Å, N6–H(6A)$\cdots$Cl(1′) 150(2)°].

55 D. R. Hamann, *Phys. Rev. B: Condens. Matter Mater. Phys.*, 1997, **16**, R10157.

56 G. Rovira, J. J. Novoa and P. Ballone, *J. Chem. Phys.*, 2001, **115**, 6406.

57 E_D and E_M correspond to the binding energy of the dimeric assembly and of the isolated monomer, respectively.

58 BSSE was estimated through the use of reference energies computed with a ghost monomer. See: A. Rosa, A. W. Ehlers, E. J. Baerends, J. G. Snijders and G. te Velde, *J. Phys. Chem.*, 1996, **100**, 5690.

59 (*a*) G. Aullón, D. Bellamy, L. Brammer, E. A. Bruton and A. G. Orpen, *Chem. Commun.*, 1998, 653; (*b*) L. Brammer, E. A Bruton and P. Sherwood, *Cryst. Growth Des.*, 2001, **1**, 277; (*c*) R. Banerjee, G. R. Desiraju, R. Mondal and J. A. K. Howard, *Chem.–Eur. J.*, 2004, **10**, 3373.

60 (*a*) V. I. Mur, *Russ. Chem. Rev.*, 1964, **33**, 92; (*b*) S. Samaritani, P. Peluso, C. Malanga and R. Menicagli, *Eur. J. Org. Chem.*, 2002, 1551.

61 (*a*) H. Zhu, Z. Yu, X. You, H. Hu and X. Huang, *J. Chem. Crystallogr.*, 1999, **29**, 239; (*b*) D. M. L. Goodgame, I. Hussain, A. J. P. White and D. J. Williams, *J. Chem. Soc., Dalton Trans.*, 1999, **29**, 2899; (*c*) K. Sivashankar, A. Ranganathan, V. R. Pedireddi and C. N. R. Rao, *J. Mol. Struct.*, 2001, **559**, 41; (*d*) J. Zhang, Z.-J. Li, Y.-H. Wen, Y. Kang, J.-K. Cheng and Y.-G. Yao, *J. Mol. Struct.*, 2004, **697**, 185; (*e*) Y.-Q. Yu, C.-Z. Lu, X. He, S.-M. Chen, Q.-Z. Zhang, L.-J. Chen and W.-B. Yang, *J. Chem. Crystallogr.*, 2004, **34**, 905; (*f*) C. Chen, C.-W. Yeh and J.-D. Chen, *Polyhedron*, 2006, **25**, 1307.

62 In ref. 61*c* is reported the formation of a coordination polymer where two endocyclic nitrogens of melamine bridge two Ag(I) ions.